



Acid-base chemistry and proton conductivity of CsHSO₄, CsH₂PO₄ and their mixtures with N-heterocycles

Aili, David; Gao, Ying; Han, Junyoung; Li, Qingfeng

Published in:
Solid State Ionics

Link to article, DOI:
[10.1016/j.ssi.2017.03.012](https://doi.org/10.1016/j.ssi.2017.03.012)

Publication date:
2017

Document Version
Peer reviewed version

[Link back to DTU Orbit](#)

Citation (APA):

Aili, D., Gao, Y., Han, J., & Li, Q. (2017). Acid-base chemistry and proton conductivity of CsHSO₄, CsH₂PO₄ and their mixtures with N-heterocycles . *Solid State Ionics*, 306, 13-19. <https://doi.org/10.1016/j.ssi.2017.03.012>

General rights

Copyright and moral rights for the publications made accessible in the public portal are retained by the authors and/or other copyright owners and it is a condition of accessing publications that users recognise and abide by the legal requirements associated with these rights.

- Users may download and print one copy of any publication from the public portal for the purpose of private study or research.
- You may not further distribute the material or use it for any profit-making activity or commercial gain
- You may freely distribute the URL identifying the publication in the public portal

If you believe that this document breaches copyright please contact us providing details, and we will remove access to the work immediately and investigate your claim.

Acid-base chemistry and proton conductivity of CsHSO₄, CsH₂PO₄ and their mixtures with *N*-heterocycles

David Aili*, Ying Gao, Junyoung Han and Qingfeng Li

*Department of Energy Conversion and Storage, Technical University of Denmark, Kemitorvet 207, DK-2800 Kgs. Lyngby, Denmark, *Corresponding author (E-mail: larda@dtu.dk)*

Abstract

Caesium hydrogen sulfate (CsHSO₄) and caesium dihydrogen phosphate (CsH₂PO₄) are solid acids that undergo superprotonic phase-transitions at about 140 and 230 °C, respectively. As a result, the proton conductivity is increased by several orders of magnitude. However, the practical operational temperature range is narrow due to decomposition of the high-conductivity phases. For CsHSO₄, it is known that this window can be extended to lower temperatures by addition of carefully selected *N*-heterocycles. The present work investigates if the same approach can be used to extend the practical operating temperature of CsH₂PO₄ as well. Binary mixtures of CsH₂PO₄ with 1,2,4-triazole, benzimidazole or imidazole were prepared by means of mechanochemical synthesis. Mixtures based on CsHSO₄ were prepared as a basis for a comparative discussion. It was found that CsHSO₄ formed organic-inorganic salts, while CsH₂PO₄ formed heterogeneous mixtures with the *N*-heterocycles due to its weaker acidity. At a *N*-heterocycle content of 30 mol%, enhanced proton conductivity was observed for both solid acids at temperatures below the superprotonic phase transitions.

Keywords: solid acid, caesium dihydrogen phosphate, composite, electrolyte, conductivity

1 Introduction

The solid acid proton conductors based on tetrahedral oxyanions comprise a family of materials that has attracted considerable attention for their potential uses as proton conducting electrolytes in the intermediate temperature range from 100 to 300 °C [1-4]. Caesium dihydrogen phosphate (CsH_2PO_4 , CHP), the mono caesium salt of phosphoric acid (H_3PO_4), is among the most thoroughly studied solid acids, showing a superprotonic phase-transition at about 230 °C [5]. Above this threshold temperature a dynamic disordered hydrogen bond network is developed, resulting in an increase in the proton conductivity by several orders of magnitude. For example, when the temperature is increased from 223 to 233 °C the proton conductivity of CHP increases from 8.5×10^{-6} to 1.8×10^{-2} S cm^{-1} [3]. Fuel cells based on CHP thin films as electrolyte show power densities as high as 400 mW cm^{-2} at 240 °C [6]. However, at temperatures above 230 °C the CHP gradually dehydrates to $\text{Cs}_2\text{H}_2\text{P}_2\text{O}_7$ and further to CsPO_3 [7]. Active humidification prevents the dehydration and stable fuel cell operation can be achieved at 235-243 °C [8]. In this connection, heterogeneous doping with alumina [9] or zirconia [10] have been found to suppress the dehydration and to stabilize the high conductivity phase. Similarly, at temperatures below the superprotonic phase transition the conductivity depends on the amount of water in the structure and particularly on strongly bound surface-water [11]. To broaden the operational temperature window to lower temperatures, incorporation of caesium hydrogen sulfate (CsHSO_4 , CHS) [12-14] or finely dispersed SiO_2 [15, 16], SrZrO_3 [17], $\text{H}_3\text{PW}_{12}\text{O}_{40}$ [18], NdPO_4 [19] or guanine [20] within the structure have proven successful.

CHS, the mono-caesium salt of sulfuric acid (H_2SO_4), shows a similar superprotonic phase transition as CHP but at a considerably lower temperature of 140 °C [21]. In terms of stability, dehydration at temperatures above the superprotonic phase transition temperature is of critical concern for CHS as well [22]. The proton conductivity of CHS at temperatures below

the superprotonic phase transition is typically in the 10^{-7} - 10^{-6} S cm⁻¹ range at 100-130 °C [21]. Several approaches to increase the proton conductivity of CHS in this temperature range have been reported throughout the years, focusing on the development of binary inorganic systems with SiO₂ [23-25], P₂O₅-SiO₂ [26], TiO₂ [27], H₃PW₁₂O₄₀ [28] or CsH₂PO₄ [12-14]. Recently, binary mixtures composed of CHS and organic *N*-heterocycles were prepared by mechanochemical synthesis and thoroughly characterized [29, 30]. For the binary compounds of CHS containing 20 mol% 1,2,4-triazole (Tz) or imidazole (Im) the conductivity reached as high as 10⁻³ S cm⁻¹ at 80 °C, which is about 3-4 orders of magnitude higher than that of the pure compounds. For the binary system with benzimidazole (BIm) the effect was considerably less pronounced. It was proposed that the acid-base interactions between the acidic CHS and basic *N*-heterocycles promote the disordering of the sulfate groups leading to enhanced proton mobility in the lower temperature regime [29, 30]. Similarly, addition of a small amount (up to 12 mol%) Im to H₂SO₄ has been found to promote the proton dissociation and generation of proton defects, ultimately leading to enhanced ion conductivity [31]. This is apparently different from phosphoric acid [32, 33], where water seems to be the only Brønsted base that can increase the concentration of ionic charge carriers as well as promote the proton mobility [34].

The proton conductivity of nominally dry phosphoric acid is remarkably high due its unique hydrogen-bond network structure, through which protons diffuse almost entirely by the Grotthuss-type mechanism at high phosphoric acid concentrations [35]. In combination with its low vapor pressure, it is therefore the most promising dopant used for high temperature polymer electrolyte membrane fuel cells based on *N*-heteroaromatic polymers [36, 37]. However, the strong adsorption of phosphoric acid on the platinum electrocatalysts at cathodic potentials results in poor performance at low currents. As discussed by Kreuer [34], replacing

phosphoric acid with CHP as the proton conducting electrolyte could be one way to enhance the kinetics for the oxygen reduction reaction.

The present work focuses on the chemical and electrochemical characteristics of binary mixtures of CHP and organic *N*-heterocycles as a model system. A set of binary mixtures composed of CHS and the *N*-heterocycles are prepared for comparison and the results are discussed in light of fundamental acid base chemistry.

2 Experimental

2.1 Materials

CsH₂PO₄ was prepared from a mixture of Cs₂CO₃ (Aldrich, 99%) and aqueous H₃PO₄ (Aldrich, 85%) with a slight over-stoichiometry of the acid. Polycrystalline CsH₂PO₄ was subsequently precipitated in methanol at room temperature. The precipitate was then filtered off and extensively washed with methanol and finally dried at 80 °C overnight.

CsHSO₄ was prepared from an equimolar mixture of Cs₂SO₄ (Aldrich, 99%) and H₂SO₄ (98%, Aldrich) in aqueous solution. CsHSO₄ was precipitated in methanol, isolated by filtration and extensively washed with methanol and dried for one week at 60 °C.

The inorganic-organic binary compounds were synthesized by blending the CsH₂PO₄ or CsHSO₄ with the *N*-heterocycles (1,2,4-triazole, benzimidazole and imidazole, Sigma-Aldrich) at different ratios, followed by solid-state ball milling at 700 rpm for 4 h, using a ball mill with an agate pot (Fritsch, 45 mL) and 10 agate balls made of tungsten carbide (10 mm in diameter). The obtained materials were stored under dry inert atmosphere in a glove-box until further use.

2.2 Characterization

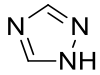
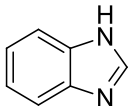
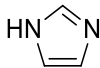
Thermogravimetric analysis (TGA) and differential thermal analysis (DTA) were performed on a Netzsch STA 409 PC under air atmosphere at $10\text{ }^{\circ}\text{C min}^{-1}$. X-ray diffraction (XRD) was carried out using a Rigaku MiniFlex 600 equipped with a Cu K_{α} X-ray source ($\lambda=1.5418\text{ \AA}$) in the range from 3° to $100^{\circ} 2\theta$. The Fourier transform infrared (FT-IR) spectra were recorded on a Perkin Elmer Spectrum Two in attenuated total reflectance (ATR) mode, using a Golden Gate high temperature heated diamond ATR top plate from Specac.

The proton conductivity was measured by electrochemical impedance spectroscopy over a frequency range of $1\text{-}10^6\text{ Hz}$ using a Princeton Versastat 4 potentiostat equipped with Versastudio software. For electrochemical characterizations, the powders were pressed into disk-shaped tablets of 13 mm diameter of varying thicknesses (around 0.5 mm). This was done by uniaxial pressing at 2000 kg cm^{-2} for 2 minutes at room temperature. In order to improve the contact between the pellet and the electrodes, a thin layer of silver paste (Loctite[®] 3863, Henkel Co.) was painted on both sides of electrolyte tablets. For the humidity control, a mixture of air and water was used as the purging gas. Water was fed to an evaporator using a Shimadzu Prominence LC-20AD water pump and the steam was converged with the air-flow, decompressed from 7 bar and controlled by a Brooks Instrument 0254 mass flow meter. At temperatures below $100\text{ }^{\circ}\text{C}$ the measurements were carried out under un-humidified air. Unless otherwise noted, the partial pressure of steam was 0.4 atm.

3 Results and discussion

Binary materials based on CHP or CHS and a set of *N*-heterocycles were prepared by mechanochemical synthesis, according to methodology previously described in the literature [18, 29]. The fundamental physicochemical properties of the *N*-heterocycles are listed in Table 1 in the order of increasing basicity in water.

Table 1 *N*-heterocycles used for the screening and their corresponding physical properties [38].

<i>N</i> -heterocycle (abbreviation)	Structure	Melting point / °C	Boiling point / °C	p <i>K</i> _{aH} ^a
1,2,4-triazole (Tz)		120-121	260	2.4
Benzimidazole (BIm)		170-172	360	5.6
Imidazole (Im)		89-91	256	6.9

^a In H₂O

The X-ray diffractograms in the range from $2\theta = 20-40^\circ$ of the binary mixtures of CHP or CHS containing 30 mol%, Tz, Im or BIm are shown in Figure 1. The XRD patterns of the binary compounds based on CHS (Figure 1a-c) were apparently different from that of the individual components indicating the formation of ionic compound with a different crystalline structure than the starting materials [29, 30]. Particularly, the main CHS peak at $2\theta = 25.1^\circ$ was found to shift to lower angles as previously reported [30]. In contrast, the XRD patterns of the binary compounds based on CHP (Figure 1d-f) were practically identical with that of CHP. The diffraction peaks originating from the *N*-heterocycles were very weak, indicating formation of an amorphous phase of the *N*-heterocycles within the crystalline CHP framework. However, as also observed for the binary compounds based on CHS, the CHP signals were shifted to lower angles in the binary compounds compared to the pure CHP. For example, the main peak of the monoclinic phase at $2\theta = 23.8^\circ$ for pure CHP [18] was shifted to about $2\theta = 23.5^\circ$ for the binary

compounds with the *N*-heterocycles, likely due to interactions with the amorphous *N*-heterocycle phase.

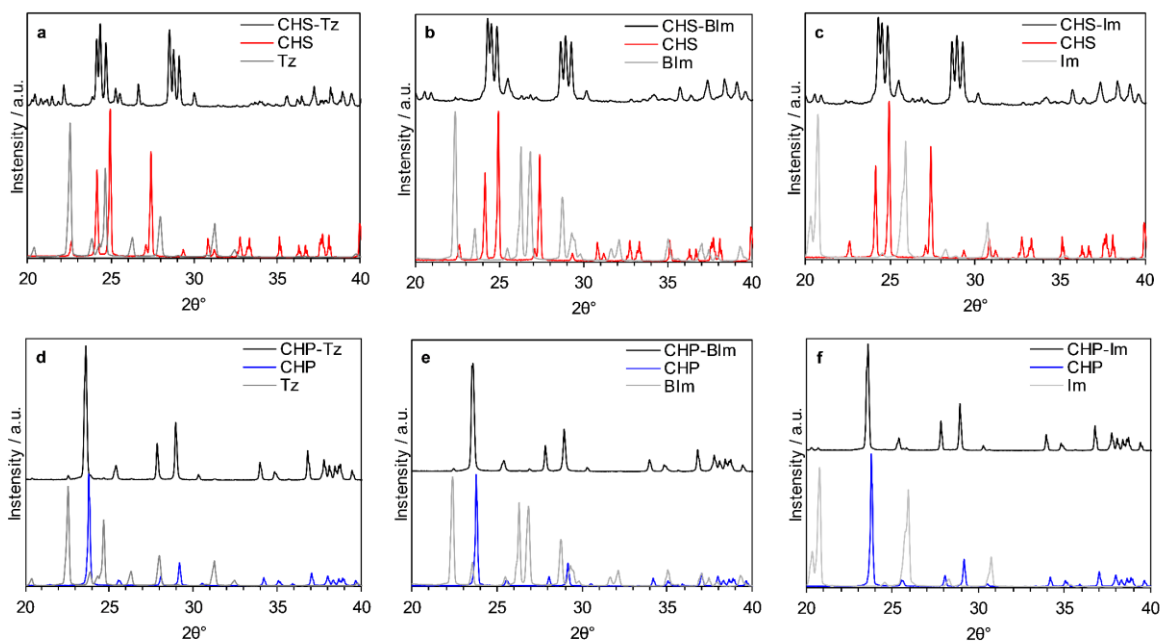


Figure 1 XRD of the binary compounds based on CHS (a-c) and CHP (d-f) containing 30 mol% Tz, BIm or Im.

The FT-IR spectra of the binary mixtures of CHP or CHS containing 30 mol%, Tz, Im or BIm are shown in Figure 2. The FT-IR spectra of pure CHS and CHP are shown for comparison, whose main spectral features have been assigned and discussed in more details [39-41]. The main absorption bands of the corresponding *N*-heterocycles are indicated by vertical dotted lines. On one hand, the FT-IR spectra of the binary mixtures of CHS showed signals that were not present in the spectra of the individual constituents (marked by + in Figure 2), indicating complete formation of homogenous inorganic-organic salts. For example, the new strong characteristic absorption band at about 1200 cm^{-1} present in all binary mixtures based on CHS corresponds to stretching modes of ionic sulfonates [40]. The strong SO_4 absorption band at 570 cm^{-1} in pure CHS [40] was shifted to lower frequencies (580 cm^{-1}) in the binary compounds

further indicating altered chemical environment of the sulfonate. Furthermore, the absorption bands at 1577, 1620 and 1586 cm^{-1} in spectra of the binary mixtures of CHS and Tz, BIm and Im, respectively, is indicative for the interaction between the two components [29, 30]. On the other hand, the spectra of the binary mixtures based on CHP showed no significantly changed spectral features compared with the individual component. However, new weak absorption bands at 504 and 525 cm^{-1} appeared indicating changed chemical environment of the phosphate anions [20].

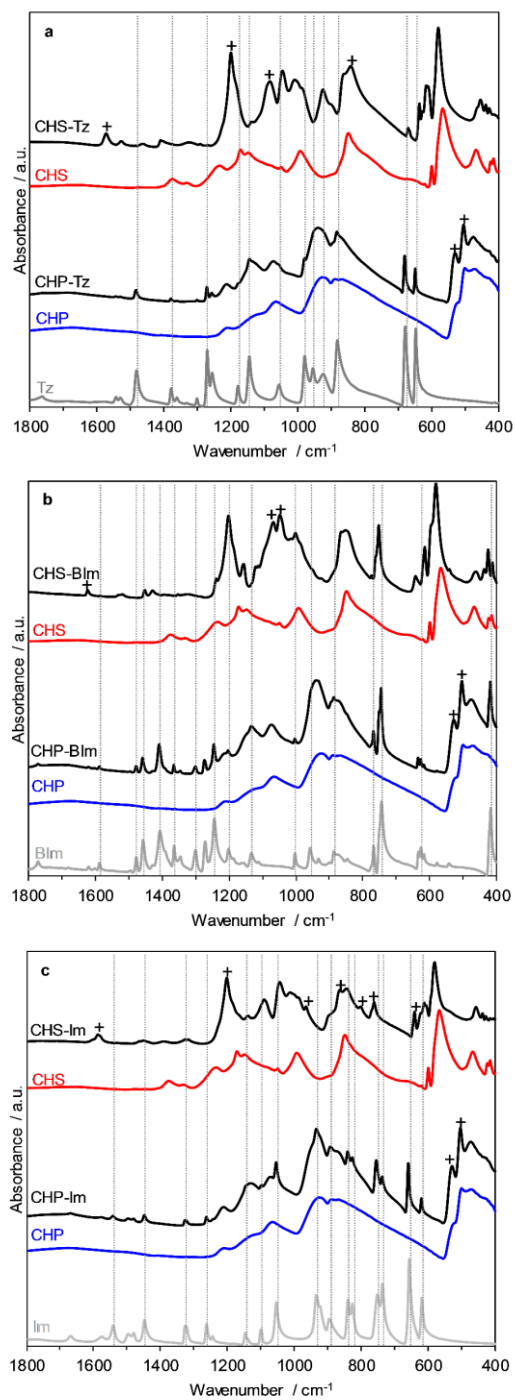


Figure 2 FT-IR spectra of the binary compounds (black lines) and of the corresponding individual components. The major absorption bands of the *N*-heterocycles are indicated by vertical lines.

Thermogravimetric analysis (TGA) in combination with differential thermal analysis (DTA) was carried out in order to obtain more information about the thermal behavior of the binary mixtures. The TGA and DTA data for the binary mixtures based on CHS and CHP are shown in Figure 3a-c and 3d-f, respectively, plotted together with the data for the corresponding individual components. The endothermic peak temperatures and the onset temperatures of the major mass loss steps are summarized in Table 2.

The dehydration of CHP occurred in two steps, with a first onset close to the superprotonic phase transition (227 °C). Tz, BIm and Im showed the first endothermic peaks at 119, 170 and 88 °C, respectively, in good agreements with the melting temperatures (see Table 1). Furthermore, endothermic peaks were recorded at 208, 284 and 220 °C, respectively, likely corresponding to the boiling. However, the major onset of weight loss for Tz, BIm and Im was about 137, 205 and 140 °C, indicating that the vapor pressure at temperatures well below the boiling temperatures is sufficiently high to result in a significant evaporation rate. The endothermic peaks of the binary mixtures based on CHP were in agreement with the peaks of the individual components, further supporting the XRD and FT-IR data.

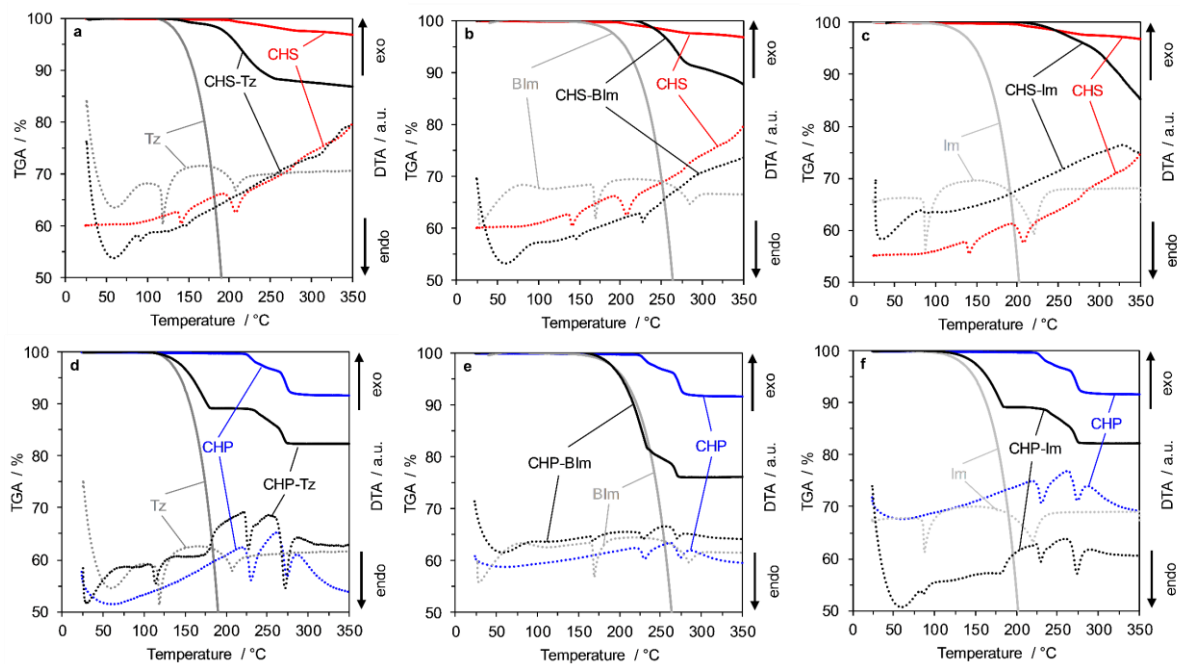


Figure 3 Thermogravimetric curves (solid lines) and differential thermal analysis data (dotted lines) for the CHS (a-c) and CHP (d-f) binary compounds containing 30 mol% Tz, BIm and Im.

Table 2 Endothermic peaks and major onsets of weight loss temperatures of CHP, CHS, Tz, Im and BIm and of the CHP and CHS binary compounds containing 30 mol% Tz, Im and BIm. Data extracted from TGA/DTA measurements at 10 °C min⁻¹.

Sample	Endothermic peaks / °C	Onsets of weight loss / °C
CHS	140, 206	197, 326
CHP	230, 273	227, 266
Tz	119, 208	137
BIm	170, 284	205
Im	88, 220	140
CHS-Tz	91	146, 190
CHS-BIm	145, 228	232, 333
CHS-Im	-	225, 297
CHP-Tz	114, 228, 271	150, 234, 263
CHP-BIm	169, 230, 271	201, 262
CHP-Im	87, 230, 275	144, 234, 269

In context of the acid-base chemistry, the results from the XRD, FT-IR and TGA/DTA studies in the present work confirm previously reported data for the mixtures based on CHS [29, 30]. The pK_a corresponding to the dissociation of HSO_4^- is 2.0 (in water), which is similar to the pK_a corresponding to the dissociation of H_3PO_4 . Consider the varied pK_{aH} values of 2.4 for Tz, 5.6 for BIm and 6.9 for Im, CHS is sufficiently acidic to interact with Tz, BIm and Im, leading to formation of extensive hydrogen bonds or eventually inorganic-organic ionic salts by complete transfer of its proton, as shown in Figure 4 (left).

The pK_a corresponding to the dissociation of H_2PO_4^- , on the other hand, is around 7.2 in water. It indicates that CHP is about 5 orders of magnitude less acidic than CHS and thus

not sufficiently acidic to protonate Tz, BIm or Im to any significant extent. Heterogeneous mixtures were thus obtained when CHP was mixed with the *N*-heterocycles, as illustrated in Figure 4 (right).

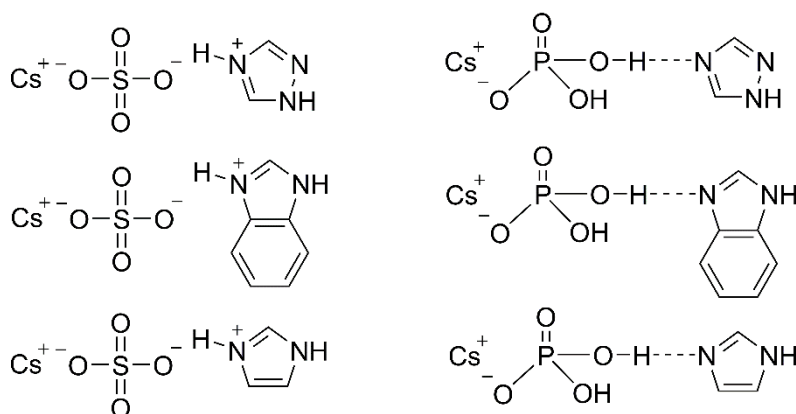


Figure 4 Chemical structures of the binary *N*-heterocycle mixtures based on CHS (left) and CHP (right).

We can now have a closer look at the TGA/DTA data in Table 2. Strong acid-base interactions between CHS and Im (strongest), BIm (medium) and Tz (weakest) result in formation of inorganic-organic salts and therefore stabilize the volatile base molecules by electrostatic interactions. As a result, the onset temperatures are found to increase by 85 °C for CHS-Im, 27 °C for CHS-BIm, and 9 °C for CHS-Tz compared to the individual *N*-heterocycle. For the CHP mixtures, however, the mismatched acidity relative to the *N*-heterocycles leads to a low degree of ionization and the thermogravimetric behavior of the volatile bases thus remains unchanged in relation to their pristine forms. The binary systems based on CHP are therefore better understood as heterogeneous composite systems, rather than homogenous mixtures.

As shown in Figure 5, the ion conductivity of pure CHS and CHP was found to increase by several orders of magnitude at about 140 and 230 °C, respectively, in good agreement with the data in the literature [5, 21]. As described previously in the literature [3, 9], the ion

conductivity of CHP and CHS showed thermal hysteresis during the heating-cooling loop. The binary mixtures of CHS and Tz or Im showed significantly enhanced conductivity at temperatures below the superprotonic phase transition of pure CHS, confirming the results reported by Oh et al. [30]. For example, the ion conductivity at 100 °C of the binary mixtures of CHS and Tz or Im was about 1.5 mS cm⁻¹, as compared with about 6 × 10⁻⁴ mS cm⁻¹ for pure CHS.

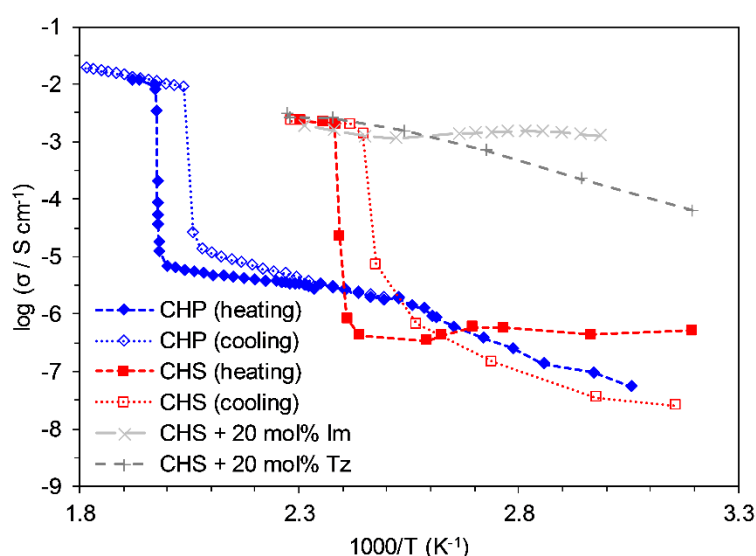


Figure 5 Conductivity of CHS doped with 20 mol% imidazole or 1,2,4-triazole measured without humidification. The conductivity of pure CHS and CHP is shown for comparison for the first heating (solid) and cooling (open) cycles.

The ion conductivity of the binary compounds composed of CHP and 30 mol% Tz, BIm or Im was recorded at temperature ranging from 50-250 °C, as shown in Figure 6a. The conductivity of the binary CHP-BIm mixture was marginally higher than that of pure CHP at temperatures below 240 °C, likely due to the high melting temperature of BIm in combination with its relatively high molecular weight [30]. In the lower temperature range, the conductivity of the binary mixtures with Tz and Im gradually increased with increasing temperature and reached

a plateau at 119 and 90 °C, respectively, i.e. at the corresponding melting temperatures of the secondary components. The conductivity remained stable at about 0.2-0.8 mS cm⁻¹ up to 174-190 °C, beyond which it started to decline due to evaporation as supported by the TGA/DTA data and the temperature dependent FT-IR spectra (Figure S1). It can thus be expected that the chemical composition as well as the conductivity of the binary CHP-Tz/Im mixtures strongly depend on the thermal history of the sample.

To assess the stability of the composite electrolytes, the conductivity of the binary mixtures with Tz and Im was recorded at 130 °C during more than 12 h as shown in Figure 6b. The conductivity of the binary composite with Im was initially slightly higher than for the corresponding sample measured during the heating scan, likely due to batch-to-batch variations. The conductivity of the binary composites of CHP containing 30 mol% Tz or Im was initially 0.7 and 1.1 mS cm⁻¹, respectively. After 12 h it had decreased to 0.3 and 0.5 mS cm⁻¹, respectively, likely due to evaporation of the *N*-heterocycles.

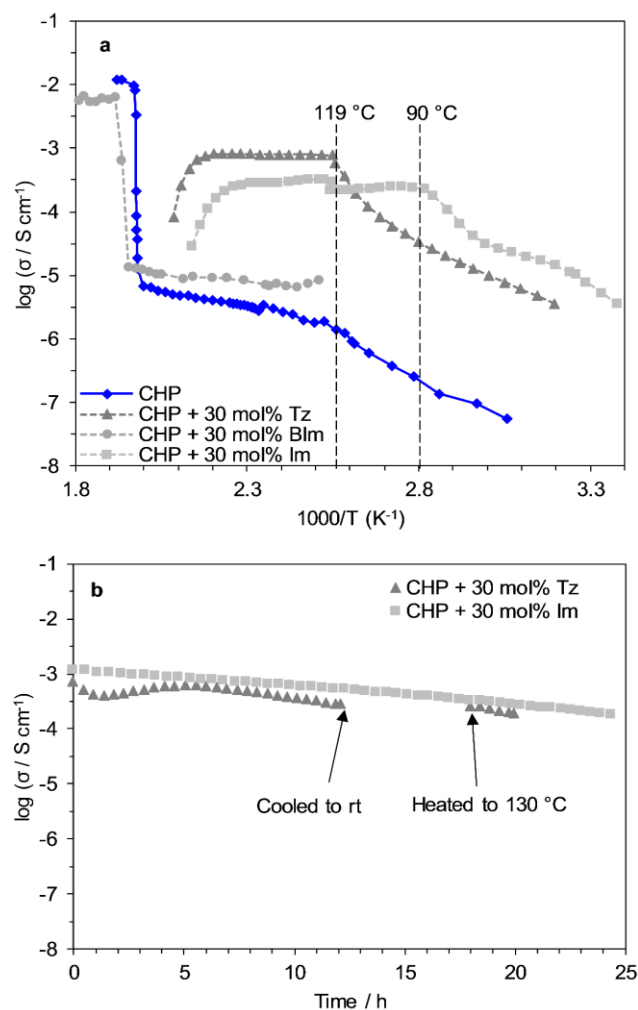


Figure 6 Conductivity of the binary compounds of CHP and 30 mol% Tz, BIm or Im as functions of temperature (a) and of the binary compounds of CHP with 30 mol% Tz or Im at 130°C as functions of time (b).

The binary mixture of CHP with Tz was chosen for further studies with respect to composition. Binary mixtures of CHP and 10, 30 and 50 mol% Tz were prepared and their conductivity is plotted as functions of temperature in Figure 7. At temperatures below the melting point of Tz, the conductivity increased gradually with increasing temperature. At 90°C the conductivity of the CHP mixture containing 30 mol% Tz was $4.5 \times 10^{-5} \text{ S cm}^{-1}$, which can be compared with $8 \times 10^{-6} \text{ S cm}^{-1}$ for pure Tz [42]. Above the melting temperature of Tz, the conductivity of the binary mixtures of CHP containing 30 and 50 mol% Tz was similar and reached around 1 mS

cm⁻¹ at 120 °C. For comparison, the ion conductivity of pure CHP and Tz at 120 °C was 1.7×10^{-6} and 1.5×10^{-3} S cm⁻¹, respectively. Even at a low Tz content, 10 mol%, the ion conductivity was significantly enhanced at 120-130 °C and reached 6×10^{-5} S cm⁻¹. For comparison, the conductivity of molten Tz increased from 2.0×10^{-3} to 2.4×10^{-3} S cm⁻¹ when the temperature was increased from 130 to 160 °C.

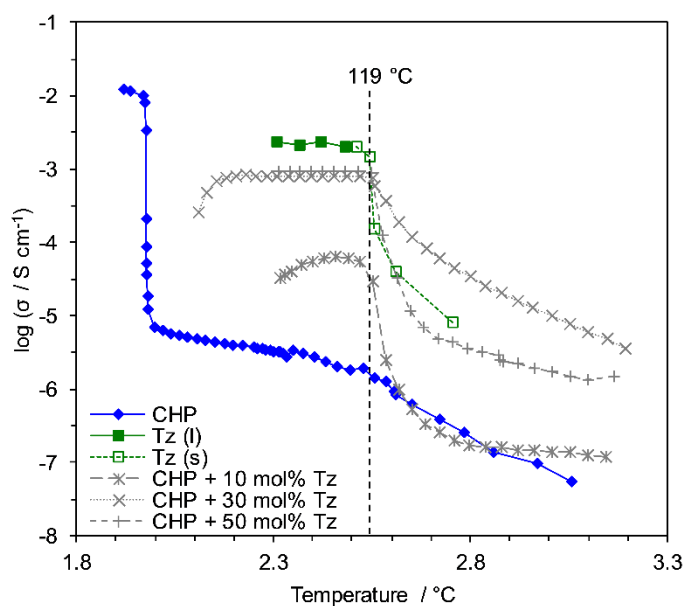


Figure 7 Conductivity of CHP mixtures containing 10, 30 and 50 mol% Tz. The conductivity of Tz in liquid (l) [42] and solid (s) state is shown for comparison.

As discussed above, the binary systems based on CHP and the *N*-heterocycles are best described as heterogeneous composite systems composed of a *N*-heterocycle phase dispersed in a structural porous matrix of CHP. In this connection, the physicochemical properties of the composite electrolyte largely depend on the structure of the composite and the interphases between the components [43]. In confined spaces, the physicochemical properties and ion conductivity behavior of *N*-heterocycles such as Im [44] or Tz [45] can be strongly modulated. In this work, it is obvious that the *N*-heterocycles dispersed in the solid acid matrix phase

provide an environment that show enhanced ion conductivity at temperatures well-below the superprotonic phase transition of CHP. This is likely due to weak hydrogen-bond interactions between CHP and the *N*-heterocycles, promoting the proton dissociation and thus the generation of proton defects, which mechanistically is an underlying process in the conduction of protons [46, 47].

4 Conclusions

Binary mixtures of CsHSO₄ and CsH₂PO₄ with 1,2,4-triazole, benzimidazole or imidazole were prepared by means of mechanochemical synthesis. XRD, TGA/DTA and FT-IR results show that CsHSO₄ formed homogenous mixtures i.e. organic-inorganic salts with the *N*-heterocycles. CsH₂PO₄ was found to be insufficiently acidic to protonate the *N*-heterocycles to any significant extent. As a result of the acid-base interaction and the developed electrostatic interactions, the CsHSO₄ mixtures with *N*-heterocycles show improved thermal stabilities with respect to the volatile basic components. Significant enhancement of proton conductivity was achieved in the temperature range lower than the superprotonic phase transition. On the other hand, no acid-base chemistry was identified for the CsH₂PO₄ mixtures where the *N*-heterocycles possess similar volatility as in their pristine form. Those binary systems are therefore best described as composites rather than homogenous mixtures. The proton conductivity of the binary mixtures based on CsH₂PO₄ was considerably enhanced at temperatures below the superprotonic phase transition of CsH₂PO₄ and below the evaporation temperatures of the *N*-heterocycle additives. This could be due to promotion of proton dissociation by the basic *N*-heterocycles or due to altered conductivity behavior of the confined *N*-heterocycles within the porous CHP matrix.

Acknowledgments

This work was financially supported by the Danish Council for Strategic Research (4M Centre).

References

- [1] T. Norby, Solid-state protonic conductors: principles, properties, progress and prospects, *Solid State Ionics* 125 (1999) 1-11.
- [2] S.M. Haile, D.A. Boysen, C.R.I. Chisholm, R.B. Merle, Solid acids as fuel cell electrolytes, *Nature* 410 (2001) 910-913.
- [3] S.M. Haile, C.R.I. Chisholm, K. Sasaki, D.A. Boysen, T. Uda, Solid acid proton conductors: from laboratory curiosities to fuel cell electrolytes, *Faraday Discuss.* 134 (2007) 17-39.
- [4] N. Mohammad, A.B. Mohamad, A.A.H. Kadhum, K.S. Loh, A review on synthesis and characterization of solid acid materials for fuel cell applications, *J. Power Sources* 322 (2016) 77-92.
- [5] A.I. Baranov, B.V. Merinov, A.V. Tregubchenko, V.P. Khiznichenko, L.A. Shuvalov, N.M. Schagina, Fast proton transport in crystals with a dynamically disordered hydrogen bond network, *Solid State Ionics* 36 (1989) 279-282.
- [6] T. Uda, S.M. Haile, Thin-membrane solid-acid fuel cell, *Electrochem. Solid-State Lett.* 8 (2005) A245-A246.
- [7] Y.K. Taninouchi, T. Uda, Y. Awakura, A. Ikeda, S.M. Haile, Dehydration behavior of the superprotonic conductor CsH_2PO_4 at moderate temperatures: 230 to 260 °C, *J. Mater. Chem.* 17 (2007) 3182-3189.
- [8] D.A. Boysen, T. Uda, C.R.I. Chisholm, S.M. Haile, High-performance solid acid fuel cells through humidity stabilization, *Science* 303 (2004) 68-70.

- [9] A.I. Baranov, V.V. Grebenev, A.N. Khodan, V.V. Dolbinina, E.P. Efremova, Optimization of superprotonic acid salts for fuel cell applications, *Solid State Ionics* 176 (2005) 2871-2874.
- [10] A.H. Jensen, Q. Li, E. Christensen, N.J. Bjerrum, Intermediate temperature fuel cell using $\text{CsH}_2\text{PO}_4/\text{ZrO}_2$ -based composite electrolytes, *J. Electrochem. Soc.* 161 (2014) F72-F76.
- [11] D.A. Boysen, S.M. Haile, H.J. Liu, R.A. Secco, High-temperature behavior of CsH_2PO_4 under both ambient and high pressure conditions, *Chem. Mater.* 15 (2003) 727-736.
- [12] T. Sugahara, A. Hayashi, K. Tadanaga, M. Tatsumisago, Characterization of proton conducting CsHSO_4 - CsH_2PO_4 ionic glasses prepared by the melt-quenching method, *Solid State Ionics* 181 (2010) 190-192.
- [13] H. Takahashi, Y. Suzuki, T. Sakuma, New phase transition in superprotonic phase of inorganic solid acid $\text{Cs}_2(\text{HSO}_4)(\text{H}_2\text{PO}_4)$, *Solid State Ionics* 285 (2016) 155-159.
- [14] I.N. Bagryantseva, V.G. Ponomareva, Proton conductivity and phase composition of mixed salts in the systems $M\text{H}_2\text{PO}_4$ - CsHSO_4 ($M = \text{Cs}, \text{K}$), *Phys. Solid State* 58 (2016) 1651-1658.
- [15] J. Otomo, N. Minagawa, C.-j. Wen, K. Eguchi, H. Takahashi, Protonic conduction of CsH_2PO_4 and its composite with silica in dry and humid atmospheres, *Solid State Ionics* 156 (2003) 357-369.
- [16] V.G. Ponomareva, E.S. Shutova, High-temperature behavior of CsH_2PO_4 and CsH_2PO_4 - SiO_2 composites, *Solid State Ionics* 178 (2007) 729-734.
- [17] G.V. Lavrova, E.S. Shutova, V.G. Ponomareva, L.A. Dunyushkina, Proton conductivity and interphase interaction in CsH_2PO_4 - SrZrO_3 composites, *Russ. J. Electrochem.* 49 (2013) 718-724.

- [18] S.-Y. Oh, E.K. Insani, V.H. Nguyen, G. Kawamura, H. Muto, M. Sakai, A. Matsuda, Mechanochemically synthesized $\text{CsH}_2\text{PO}_4\text{-H}_3\text{PW}_{12}\text{O}_{40}$ composites as proton-conducting electrolytes for fuel cell systems in a dry atmosphere, *Sci. Technol. Adv. Mater.* 12 (2011) 034402.
- [19] T. Anfimova, A.H. Jensen, E. Christensen, J.O. Jensen, N.J. Bjerrum, Q. Li, $\text{CsH}_2\text{PO}_4/\text{NdPO}_4$ composites as proton conducting electrolytes for intermediate temperature fuel cells, *J. Electrochem. Soc.* 162 (2015) F436-F441.
- [20] S.-y. Oh, G. Kawamura, H. Muto, A. Matsuda, Mechanochemical synthesis of proton conductive composites derived from cesium dihydrogen phosphate and guanine, *Solid State Ionics* 225 (2012) 223-227.
- [21] A.I. Baranov, L.A. Shuvalov, N.M. Shchagina, Superior conductivity and phase transitions in CsHSO_4 and CsHSeO_4 crystals, *JETP Lett.* 36 (1982) 459-462.
- [22] R.B. Merle, C.R.I. Chisholm, D.A. Boysen, S.M. Haile, Instability of sulfate and selenate solid acids in fuel cell environments, *Energy Fuels* 17 (2003) 210-215.
- [23] V.G. Ponomareva, N.F. Uvarov, G.V. Lavrova, E.F. Hairetdinov, Composite protonic solid electrolytes in the $\text{CsHSO}_4\text{-SiO}_2$ system, *Solid State Ionics* 90 (1996) 161-166.
- [24] S.Q. Wang, J. Otomo, M. Ogura, C. Wen, H. Nagamoto, H. Takahashi, Preparation and characterization of proton-conducting $\text{CsHSO}_4\text{-SiO}_2$ nanocomposite electrolyte membranes, *Solid State Ionics* 176 (2005) 755-760.
- [25] M. Saito, Y. Nozaki, H. Tokuno, N. Sakai, J. Kuwano, Proton conduction in $\text{CsHSO}_4\text{-mesoporous silica}$ composite electrolytes, *Solid State Ionics* 180 (2009) 575-579.
- [26] M. Tatsumisago, T. Tezuka, A. Hayashi, K. Tadanaga, Preparation of proton conductive composites with cesium hydrogen sulfate and phosphosilicate gel, *Solid State Ionics* 176 (2005) 2909-2912.

- [27] H. Muroyama, T. Matsui, R. Kikuchi, K. Eguchi, Composite effect on the structure and proton conductivity for CsHSO₄ electrolytes at intermediate temperatures, *J. Electrochem. Soc.* 153 (2006) A1077-A1080.
- [28] Y. Daiko, V.H. Nguyen, T. Yazawa, H. Muto, M. Sakai, A. Matsuda, Phase transition and proton conductivity of CsHSO₄-WPA composites prepared by mechanical milling, *Solid State Ionics* 181 (2010) 183-186.
- [29] S.-Y. Oh, T. Yoshida, G. Kawamura, H. Muto, A. Matsuda, Solid-state mechanochemical synthesis of CsHSO₄ and 1,2,4-triazole inorganic-organic composite electrolytes for dry fuel cells, *Electrochim. Acta* 56 (2011) 2364-2371.
- [30] S.-Y. Oh, G. Kawamura, H. Muto, A. Matsuda, Anhydrous protic conduction of mechanochemically synthesized CsHSO₄-azole-derived composites, *Electrochim. Acta* 75 (2012) 11-19.
- [31] K.-D. Kreuer, A. Fuchs, M. Ise, M. Spaeth, J. Maier, Imidazole and pyrazole-based proton conducting polymers and liquids, *Electrochim. Acta* 43 (1998) 1281-1288.
- [32] A. Schechter, R.F. Savinell, Imidazole and 1-methyl imidazole in phosphoric acid doped polybenzimidazole, electrolyte for fuel cells, *Solid State Ionics* 147 (2002) 181-187.
- [33] L. Vilčiauskas, M.E. Tuckerman, J.P. Melchior, G. Bester, K.-D. Kreuer, First principles molecular dynamics study of proton dynamics and transport in phosphoric acid/imidazole (2:1) system, *Solid State Ionics* 252 (2013) 34-39.
- [34] K.-D. Kreuer, Ion conducting membranes for fuel cells and other electrochemical devices, *Chem. Mater.* 26 (2014) 361-380.
- [35] L. Vilčiauskas, M.E. Tuckerman, G. Bester, S.J. Paddison, K.-D. Kreuer, The mechanism of proton conduction in phosphoric acid, *Nat. Chem.* 4 (2012) 461-466.

- [36] Q. Li, J.O. Jensen, R.F. Savinell, N.J. Bjerrum, High temperature proton exchange membranes based on polybenzimidazoles for fuel cells, *Prog. Polym. Sci.* 34 (2009) 449-477.
- [37] J.K. Kallitsis, M. Geormezi, S.G. Neophytides, Polymer electrolyte membranes for high-temperature fuel cells based on aromatic polyethers bearing pyridine units, *Polym. Int.* 58 (2009) 1226-1233.
- [38] Q. Li, D. Aili, R.F. Savinell, J.O. Jensen, Acid–base chemistry and proton conductivity, in: Q. Li, D. Aili, H.A. Hjuler, J.O. Jensen (Eds.), *High temperature polymer electrolyte membrane fuel cells: Approaches, status, and perspectives*, Springer International Publishing, Cham, 2016, pp. 37-57.
- [39] B. Marchon, A. Novak, Vibrational study of CsH_2PO_4 and CsD_2PO_4 single crystals, *J. Chem. Phys.* 78 (1983) 2105-2120.
- [40] J. Baran, M.K. Marchewka, Vibrational investigation of phase transitions in CsHSO_4 crystal, *J. Mol. Struct.* 614 (2002) 133-149.
- [41] P. Colomban, M. Pham-Thi, A. Novak, Influence of thermal and mechanical treatment and of water on structural phase transitions in CsHSO_4 , *Solid State Ionics* 24 (1987) 193-203.
- [42] S.W. Li, Z. Zhou, Y.L. Zhang, M.L. Liu, W. Li, 1H-1,2,4-triazole: An effective solvent for proton-conducting electrolytes, *Chem. Mater.* 17 (2005) 5884-5886.
- [43] V. Ponomareva, G. Lavrova, Controlling the proton transport properties of solid acids via structural and microstructural modification, *J. Solid State Electrochem.* 15 (2011) 213-221.
- [44] S. Bureekaew, S. Horike, M. Higuchi, M. Mizuno, T. Kawamura, D. Tanaka, N. Yanai, S. Kitagawa, One-dimensional imidazole aggregate in aluminium porous coordination polymers with high proton conductivity, *Nat. Mater.* 8 (2009) 831-836.

- [45] J.A. Hurd, R. Vaidhyanathan, V. Thangadurai, C.I. Ratcliffe, I.L. Moudrakovski, G.K.H. Shimizu, Anhydrous proton conduction at 150 degrees C in a crystalline metal-organic framework, *Nat. Chem.* 1 (2009) 705-710.
- [46] T. Dippel, K.-D. Kreuer, J.C. Lassègues, D. Rodriguez, Proton conductivity in fused phosphoric acid; A $^1\text{H}/^{31}\text{P}$ PFG-NMR and QNS study, *Solid State Ionics* 61 (1993) 41-46.
- [47] T. Dippel, N. Hainovsky, K.-D. Kreuer, W. Munch, J. Maier, Hydrogen bonding, lattice dynamics and fast protonic conductivity, *Ferroelectrics* 167 (1995) 59-66.